Hindawi
Journal of Electrical and Computer Engineering
Volume 2021, Article ID 5516909, 13 pages
https://doi.org/10.1155/2021/5516909

Research Article

Wind Power Prediction considering Ramping Events Based on Generative Adversarial Network

Qiyue Huang

Ningbo Polytechnic, Ningbo 315800, China

Correspondence should be addressed to Qiyue Huang; 839539199@qq.com

Received 19 February 2021; Revised 9 July 2021; Accepted 14 August 2021; Published 21 October 2021

Academic Editor: Ping-Feng Pai

In view of the growing depletion of traditional fossil fuels and their adverse impact on natural environment, wind energy has gained increasing popularity across the globe. Characterized by wide distribution, low cost, and well-rounded technology, it has achieved fast-growing installed capacity in recent years. However, wind power is volatile and random in nature and the power ramping events caused by extreme weather always threaten the safe, stable, and economic operation of the power grid. To address the problems of insufficient sample data and low prediction accuracy in existing ramping prediction methods, a new way of wind power prediction considering ramping events based on Generative Adversarial Network (GAN) is proposed. First of all, the ramping events get identified and separated from the database of historical wind power, and the feature set of historical ramping events is then extracted according to the waveform and meteorological factors. Taking the feature set which integrates similar feature with historical one as the input of GAN, the simulated ramping data are continuously produced through the adversarial training of the generator and discriminator, thus enriching the ramping database. After that, the expanded ramping database can be applied to predict the ramping power through the LSTM model. An experiment based on the wind power dataset in a certain area of northwest China further verifies the effectiveness and superiority of this method compared with traditional ones.

1. Introduction

Energy powers the progress of human society. It brings people abundant material comforts and enjoyment. However, in the meantime, it may also cause serious environmental pollution to the earth. For example, traditional fossil fuels produce greenhouse gases such as carbon dioxide and sulfur oxides and toxic heavy metal particles such as mercury. Apart from that, fossil energy is exhaustible and faces the threat of resource depletion. Therefore, renewable clean energy has become the focus of research at home and abroad [1]. Wind energy, featured by large reserves, wide distribution, little pollution, and well-rounded technology, is widely favored among the power system [2]. However, it can be easily affected by wind speed, which is naturally random and intermittent, unstable, and difficult to control [3]. Especially the wind power ramping events occurring in extreme weather have posed great challenges to the safe and stable operation of power grid. Wind power ramping events here refer to the large fluctuation of output power in a short time caused by climate change happening in wind power stations, which may lead to large fluctuation of system frequency and even serious blackouts afterwards [4]. For this reason, improving the prediction accuracy of wind power is of great significance to the regular service of power system [5].

Wind power ramping prediction can be divided into direct prediction and indirect prediction [6]. The former is to directly predict the characteristics of ramping events according to the recognition mechanism trained by historical data [7]. The latter refers to the detection and identification based on the wind power prediction method using the definition of ramping [8–11]. Zheng and Kusiak [12] predicted the ramp rate of wind power directly based on data mining algorithm and compared the prediction performance of five algorithms from different time scales. Zareipour et al. [13] introduced an SVM-based trainer on the basis of historical data to directly classify and predict the

ramping range of wind power. Cui et al. [14] used statistical models to analyze the probability distribution of ramp amplitude, rate, and duration of wind power ramping time at different time scales. Besides, Mingjian et al. [15] also decomposed the original ramp power considering the strong tracking and prediction ability of Atomic Sparse Decomposition (ASD) to nonstationary signals, and the decomposed atomic components are self-predicted. Ouyang et al. [16] proposed a prediction method of correcting wind power according to the similar characteristics of the same type of ramping event under the same meteorological conditions. The direct prediction method is intuitive and accurate, but it requires a lot of historical data as the training model [17]. However, wind power ramping events are part of low-probability events and the lack of historical data restricts the development of this method.

In this paper, a wind power prediction method considering ramping events based on Generative Adversarial Network (GAN) is proposed. According to its definition, the set of ramping events is separated from historical wind power data. In consideration of meteorological factors, the historical ramping feature set is obtained after feature extraction. In order to enrich the number of samples, GAN is used to generate more simulated ramping data. GAN is composed of two parts: the generator and the discriminator. The generator continuously produces simulated ramping data according to the input feature set. The discriminator is designed to distinguish whether the data image is historical data or simulated data. Through the adversarial training of generator and discriminator, the authenticity of simulated ramping images is continuously improved. Adversarial training means that the generator generates simulated data similar to historical data, while the discriminator tries to distinguish historical data from simulated data. When the feature distribution of the simulated data image generated by the generator is basically the same as that of the historical data and the discriminator cannot distinguish it, the training is finally completed. Simulated ramping data are then added to the historical set to realize the expansion of the database. Then, re-extraction of the feature set is achieved by using it as the input of the LSTM neural network to predict the power of ramping events. Taking the wind power dataset of a certain region in Northwest China as the basis, the feasibility of the proposed method is verified through simulated experiments.

2. Characteristics Analysis of Wind Power Ramping Events

Wind power ramping events refer to the large fluctuation of wind power in a short time when wind farms are affected by extreme weather. They pose a serious threat to the quality of the power grid and the safe and stable operation of the system and even cause problems such as frequency instability and load shedding [18]. Ramping events are divided into ramping up and ramping down. When low-altitude rapids, thunderstorm, or typhoon happens, the power of the wind farm will increase sharply in a short time and therefore ramping-up events will occur. Ramping down comes when some wind turbines gradually quit operation due to weather reasons, and the power of the wind farm drops sharply in a short period of time. This chapter is to conduct qualitative and quantitative analysis on ramping events, summarize the evaluation indexes of commonly used prediction methods, and lay a theoretical foundation for the research on wind power ramping prediction methods based on Generative Adversarial Network.

2.1. Features of Ramping Events. The ramping events are identified, and the historical ramping dataset is obtained. Because of the volatility and randomness of wind power, not every power fluctuation corresponds to a ramping event. The definition of valid ramping events in this paper is expressed in the following formula:

$$\begin{cases} p_i - p_j > 0.15P_{GN}, \\ t_i - t_j < 4h, \end{cases} \tag{1}$$

where P_{GN} stands for the rated power of the wind farm, P_i indicates the power of wind farm at the moment t_i, and P_j means the power of wind farm at the moment t_j.

It can be seen that if the wind power is climbing 20% up or down 15% of the rated power within 4 hours, it is judged as a valid ramping event. With this method, all the ramping events in the historical data are extracted, and the set of ramping events is constructed as $\{E_1, E_2, E_3, \ldots, E_L\}$.

After obtaining the set of ramping events, waveform and corresponding meteorological characteristics are extracted. Since the standard units and dimensions are different when it comes to meteorological factors and wind power and the numerical values differ greatly, normalization is urgently needed for calculation. The formula is as follows:

$$y^* = \frac{y - y_{\min}}{y_{\max} - y_{\min}}, \tag{2}$$

where y signifies the value to be normalized and $y_{\max}$ and $y_{\min}$ denote the corresponding maximum and minimum values.

The waveform feature of normalized ramping power is extracted [19], and then seven characteristic values are defined, as shown in Figure 1. ΔP_l signifies the power difference between the maximum power and the minimum power on the left side, ΔP_r stands for the power difference between the maximum power and the minimum power on the right side, Δt_l means the time difference when the power rises rapidly, Δt_r means the time difference when the power decreases rapidly, $\Delta P_l/\Delta t_l$ is the rate of ramping up, $\Delta P_r/\Delta t_r$ is the rate of ramping down, and Δt represents the time of ramping process.

After normalizing the three typical meteorological factors, namely, temperature, wind speed, and humidity, the historical data feature set D is formed, together with the feature set extracted from the waveform. The set is as follows:

$$D = \left\{ \frac{\Delta P_l, \Delta P_r, \Delta t_l, \Delta t_r, \Delta P_l/\Delta t_l, \Delta P_r}{\Delta t_r, \Delta t, T_e, V_w, H} \right\}, \tag{3}$$

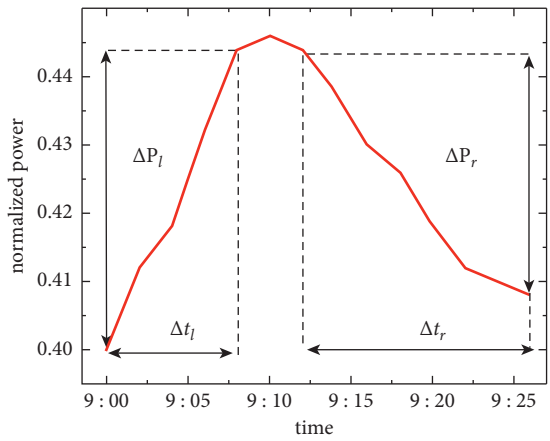

Figure 1: Characteristic values of ramping power.

where $\Delta P_l, \Delta P_r, \Delta t_l, \Delta t_r, \Delta P_l/\Delta t_l, \Delta P_r/\Delta t_r$, and Δt represent seven characteristic values of wind power waveform. Among them, T_e, V_w, and H indicate temperature, wind speed, and humidity, respectively.

2.2. Evaluation Index System. There are two evaluation indexes for wind power ramping prediction, namely, the prediction accuracy of ramping events and the prediction accuracy of power waveform [20, 21]. The accuracy of ramping events refers to whether the prediction results are consistent with the actual observation results without false positives and false negatives [22]. The prediction results are shown in Table 1.

In Table 1, TP refers to the predicted and actual occurrence of ramp events; FN means that the event is predicted not to happen but actually happens, that is, false negatives; TN signifies predicted and actual nonoccurrence of ramp events; and FP indicates that the event is predicted to happen but actually not happens, in other words, false positives [23, 24]. The prediction result is represented by N_{TP}, N_{FN}, N_{TN}, and N_{FP}. Common evaluation indexes of the accuracy of ramping prediction results are shown in formulas (4)–(6):

$$P_R = \frac{N_{\mathrm{TP}}}{N_{\mathrm{TP}} + N_{\mathrm{FP}}}, \tag{4}$$

$$R_R = \frac{N_{\mathrm{TP}}}{N_{\mathrm{TP}} + N_{\mathrm{FN}}}, \tag{5}$$

$$C_{\mathrm{SI}} = \frac{N_{\mathrm{TP}}}{N_{\mathrm{TP}} + N_{\mathrm{FN}} + N_{\mathrm{FP}}}, \tag{6}$$

where P_R stands for the precision rate, indicating the probability of the event which is predicted to happen but actually not happens; R_R means the recall rate, indicating the probability of the actual ramping event which is correctly predicted; and C_{SI} shows the critical success index, which indicates whether the prediction result is valid.

The accuracy of the ramping power waveform refers to the consistency between the predicted waveform and the actual waveform [25]. Because of the randomness and volatility of wind power and the limitations of prediction models and methods, there are inevitable errors in wind power prediction. For this reason, selecting an appropriate prediction error model is the premise and basis for quantitative analysis and verification of various evaluation indexes [26]. In this paper, Min–Max standardization is adopted to conduct linear transformation of the original data to limit the data size to [0, 1], using the normal distribution model as the basis of analysis. To evaluate the prediction accuracy of the model, mean absolute error (MAE) is applied as the standard [27]. The formula is as follows:

Table 1: Prediction results of wind power ramping events.

Predicted results	Actual results	
	Happen	Not happen
Happen	True positives (TP)	False positives (FP)
Not happen	False negatives (FN)	True negatives (TN)

$$\mathrm{MAE} = \frac{1}{n}\sum_{i=1}^{n}\left|y_t' - y_t\right|, \tag{7}$$

where n represents the number of test samples and y_t' and y_t represent the predicted power and real power at time t, respectively.

3. Prediction Model Based on Generative Adversarial Network

3.1. Flowchart of Prediction. In light of the problems of low accuracy and poor reliability caused by insufficient ramping samples in the traditional method, a new prediction method based on Generative Adversarial Network is proposed. The model first collects historical wind power data and corresponding meteorological feature set. Through ramping detection, the effective ramping events are determined and the historical ramping dataset is formed. According to the definition of ramping events, seven main characteristics of them are extracted, and the three meteorological characteristics of wind speed, temperature, and humidity are combined to obtain the historical ramping feature set. A feature set which integrates similar feature values with it is used as the input of GAN. Through the adversarial training of the generator and the discriminator, simulated ramping data with high similarity to historical climbing data are generated. It can greatly expand the number of samples while ensuring the climbing characteristics and solve the problem of insufficient input samples. The expanded dataset is refeatured and input to the LSTM neural network to produce the predicted waveform value of the ramping power. The specific workflow is shown in Figure 2.

3.2. The Structure of GAN. Generative adversarial network is used to generate simulated ramping data, which is an important part of the proposed power prediction scheme. It consists of a generator G and a discriminator D. The

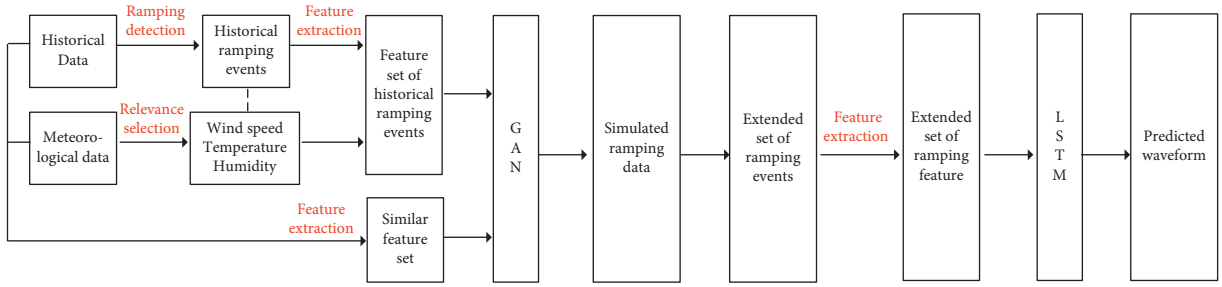

Figure 2: The flowchart of proposed prediction mode.

generator is composed of two parts: encoder and decoder. The feature set of historical ramping events is sent to the encoder to extract image features. Then, the new coding features and historical data are transmitted into the decoder in series. The decoder can generate different types of simulated ramping data by combining different feature information. The simulated ramping data and the historical data are mixed as a dataset, which is then input to the discriminator D. The discriminator distinguishes whether the data source is historical data or simulated data. Through the adversarial training, the similarity between the simulated data and the historical data is continuously improved, thus ensuring the reliability of the simulated database. The specific workflow is shown in Figure 3.

The structures of the generator G and the discriminator D are shown in Figures 4 and 5, respectively. At the core of the generator G, which is demonstrated in Figure 4, two convolutional layers with 3×3 kernels and 64 feature maps are used, followed by batch-normalization layers and ReLU as the activation function. To distinguish historical data from simulated data, a discriminator network is trained, as is illustrated in Figure 5. Here, we use Leaky ReLU activation and avoid max-pooling throughout the network. Also, the discriminator D is trained to handle the maximization problem. It includes eight convolutional layers with an increasing number of filter kernels. Strided convolutions are used to reduce the image resolution each time the number of features is doubled. Two dense layers and a final sigmoid activation function are designed to obtain a probability for sample classification. After alternatively training D and G, the output of the discriminator is stable at about 0.5. As a result, the discriminator cannot recognize whether the input data are from the historical dataset or not when the network training ends. The cost function $V(D,G)$ between the generator and the discriminator is as follows:

$$\min_G \max_D V(D,G) = E_{x\sim p_d(x)}[\log D(x)] + E_{z\sim p_z(z)}[\log(1 - D(G(z)))]. \tag{8}$$

Among them, the real ramping data x follow the data distribution $p_d(x)$ and noise z obeys Gaussian distribution. Traditional Generative Adversarial Network faces the problem of unstable training process and uncontrollable images resulted from that. To solve it, a common method is used to restrict the network and to introduce conditional variables y in the modeling process to guide the data generation process. The cost function is shown in the following formula:

$$\min_G \max_D V(D,G) = E_{x,y\sim p_d(x,y)}[\log D(x,y)] + E_{z\sim p_z(z),y\sim p_y(y)}[\log(1 - D(G(z,y),y))]. \tag{9}$$

3.3. Model Learning. Given any wind power ramping waveform diagram, its corresponding characteristic value is y^p. The proposed model includes two types: adversarial loss and content loss. Among them, adversarial loss refers to the image x', generated by the original ramp image x through the Generative Adversarial Network. Content loss refers to ensuring the consistency between the generated image and the original image through L1 loss.

Adversarial loss signifies the loss function of generator G and discriminator D in the Generative Adversarial Network. The role of generator G is to create a new ramping image through the new feature quantity and the historical data. Discriminator D is mainly used to distinguish the historical data from the simulated data. Its input contains historical samples and simulated samples of generator. Adversarial training between the generator and the discriminator can continuously improve the similarity between them, thus ensuring the diversity of the database of ramping events. The loss function between the generator and discriminator is

$$\min_G \max_D L(D,G) = E_{x,y^p\sim p_d(x,y^p)}[\log D(x,y^p)] + E_{x,y^p\sim p_d(x,y^p)}[\log(1 - D(G(x,y^p),y^p))]. \tag{10}$$

3.4. LSTM Neutral Network. Long short-term memory (LSTM) network is a special cyclic neural network, which has the advantages of better information storage and more accurate access to historical information [28]. It can avoid the gradient disappearance in RNN network and is widely applied in the processing of long time series [29–32]. In addition to the external self-circulation module, one Cell is added, which contains multiple storage units and three different "gates": input gate, forgetting gate, and output gate. The three gates are nonlinear units used to control historical information, collect external data, and filter internal data [33–35]. This paper uses LSTM neural network algorithm as the power prediction model.

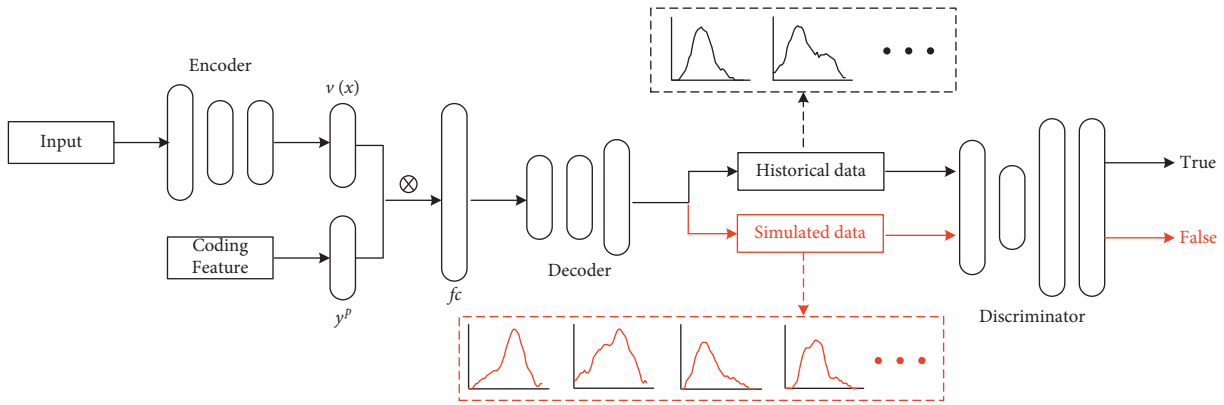

Figure 3: The flowchart of Generative Adversarial Network.

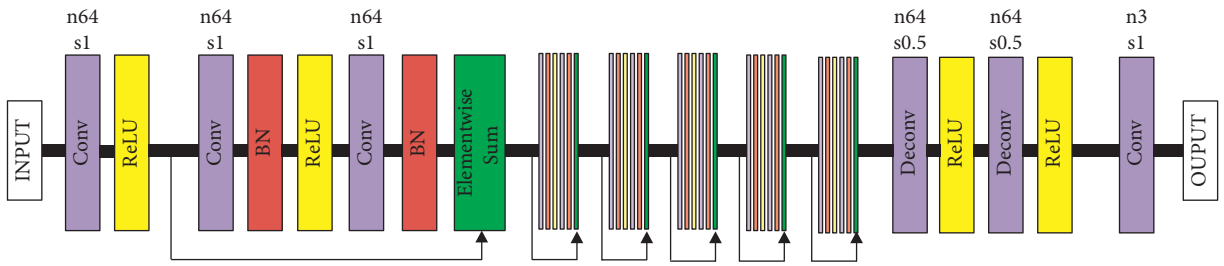

Figure 4: Neural network architecture of the generator G with corresponding numbers of feature maps (n) and stride (s) indicated for each convolutional layer.

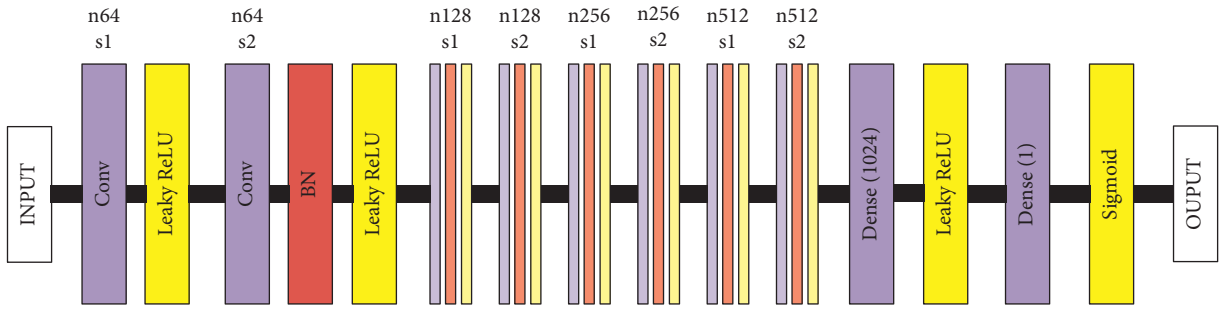

Figure 5: Neural network architecture of the discriminator D with corresponding numbers of feature maps (n) and stride (s) indicated for each convolutional layer.

4. Experimental Results and Analysis

In order to verify the effectiveness of the proposed wind power ramping prediction model based on Generative Adversarial Network, a sample dataset of a certain area in Northwest China is selected as a study case. Also, in order to make the training of the model stable, the encoder contains five convolution layers and the decoder contains seven deconvolution layers. There is a full connection layer between the encoder and the decoder. The discriminator consists of four convolution layers and two fully connected layers. In order to balance time and efficiency, VGG16 is used as each subconvolutional neural network. During training, the historical ramping image and the simulated ramping image are employed simultaneously. The experimental code is completed in TensorFlow framework.

4.1. Similarity Comparison between Simulated and Historical Data. To quantitively evaluate how similar historical ramping event data and GAN-generated data are, a method is adopted to calculate the level of similarity between historical data and simulated ones and to ensure the feasibility of power prediction. The data P are regarded as the set of feature points p_i, and the data Q are the set of feature points q_j. Each feature point p_i is used to match the corresponding q_j. The formula is as follows:

$$u_q = \frac{1}{N}\sum_j q_j, \tag{11}$$

$$d_{ij} = \left(1 - \frac{(p_i - u_q)}{\|p_i - u_q\|_2}\frac{(q_j - u_q)}{\|q_j - u_q\|_2}\right), \tag{12}$$

$$\mathrm{CX}\left(p_i, q_j\right) = \frac{e^{1-d_{ij}/h}}{\sum_k e^{1-d_{ik}/h}}, \tag{13}$$

$$\mathrm{CX}(P, Q) = \frac{1}{N}\sum_j \max_i \mathrm{CX}\left(p_i, q_j\right), \tag{14}$$

where d_{ij} is defined as the cosine distance of feature points p_i and q_j and h represents bandwidth parameter.

The distance scale is transformed into the similarity scale by exponential operation, and the standardized similarity scale is verified as shown in formulas (13) and (14). With CX (P, Q) ranging from 0 to 1, the level of similarity of the two images is indicated. After comparing the similarity between simulated data and historical ones, the results are derived as shown in Table 2. We can find that the similarity value is stable at 0.9–1, which proves that historical ramping event data and GAN-generated data are highly similar. The experiment shows that it is feasible to expand the historical climbing database by adopting simulated data.

4.2. Experiments on Different Proportions of Simulated Data. To present the actual number of simulated data and historical data and to analyze the error rate of simulated data, we made some experiments to verify the reliability. By increasing the proportion of simulated data, the reliability of power prediction is calculated. A dataset with 1000 historical ramping events and a dataset with 100 historical ramping events are used as the input of the predictive model, and the proportion of simulated data is changed from 0% to 90%. Then, MAE is calculated in Table 3.

It can be seen that the accuracy of prediction will be gradually improved by increasing the number of simulated data in the historical data. However, when the simulated data are too large, the accuracy of the prediction algorithm will be limited to a certain extent. Also, when the simulated data are from 70% to 80%, the effect of the promotion algorithm is the best. When insufficient sample data (the number of historical ramping data is 100) are adopted, it can be seen that the prediction accuracy is continuously improved and the speed of improvement is faster through GAN. When the number of historical ramping data is 1000, which is relatively sufficient, the prediction accuracy is also improved, but the improvement effect is not obvious with the increase in the proportion of generative data. When 1000 historical data and 0 simulated data are used as input, the predicted MAE error is 69, and when 100 historical data and 900 simulated data are used as input, the predicted MAE error is 81.3. It can be seen that simulated data are not as effective as real sample data when used as training samples. However, when sufficient historical data are not available, data generation is still an effective method to improve the forecasting effect.

4.3. Evaluation of Ramping Events Prediction. The ramping data of wind farms in recent years are selected for experiments. In order to ensure the quantity of ramping data and obtain a reasonable wind power prediction dataset, the model is divided into the following parts according to the steps in Figure 6.

At present, SVR, BP, and Elman neural networks have been widely used for wind farm prediction. Based on structural risk minimization, SVR has strong robustness [36]. BP is a classical neural network, which has a fast learning speed and is widely used in many fields [37]. The structure of Elman neural network is similar to BP, but the output of its hidden layer is connected with the input, which plays an important role in the global optimization of the network [38–40]. In this paper, a wind power ramping prediction model based on GAN is proposed and established, compared with the previous methods mentioned. In the sample set, 500 ramping data and 500 nonramping data are chosen for three groups of experiments. To evaluate the effect of ramping events' prediction, P_R, R_R, and C_{SI} are calculated, respectively [41]. The results obtained are shown in Table 4.

LSTM, SVR, BP, and Elman are used to predict the ramping events. It can be found that the LSTM method has the highest prediction accuracy, which is approximately 99%, while the accuracy of other methods is only about 90%. When Generative Adversarial Network is adopted to generate data, the addition of analog data will not reduce, but will improve the prediction accuracy. The simulation results have proven the prediction accuracy of wind power prediction algorithm based on Generative Adversarial Network in ramping events.

4.4. Evaluation of Power Waveform Prediction. In order to verify the effectiveness of the algorithm of Generative Adversarial Network in power waveform prediction, the proposed model is compared with the traditional SVR, BP, and Elman power prediction models. Then, MAE is calculated, respectively, to predict and evaluate ramp events. The result is shown in Table 5.

As can be seen in Table 5, the LSTM prediction algorithm has the smallest error and a higher accuracy. The prediction model generated by the adversarial network algorithm has significantly improved the prediction accuracy [42]. The simulation experiment results prove that the wind power prediction algorithm based on the Generative Adversarial Network realizes accurate prediction on ramping power waveform. The following figures show the comparisons of power waveform prediction.

It can be seen that the power prediction waveform based on the Generative Adversarial Network algorithm shares the most similarity to the real waveform in Figures 7–9.

4.5. Evaluation of Prediction of Different Confidence Levels. Figures 10–12 show the predicted power fluctuation range before and after the Generative Adversarial Network algorithm. In order to quantitatively describe the application effect of probability density function of different wind power prediction errors, the evaluation results of prediction with confidence levels of 90%, 80%, and 70% are calculated within the fluctuation range of wind power. It can be observed that the Generative Adversarial Network can significantly reduce

Table 2: The similarity between simulated data and historical data.

Group		CX(P,Q)		
		Historical data	Simulated data	Nonramping data
Historical data	#1	1	0.9673	0.1812
	#2	1	0.9781	0.1645
	#3	1	0.9787	0.2413
	#4	1	0.9948	0.2107
	#5	1	0.9307	0.1814
	#6	1	0.9152	0.1169
	#7	1	0.9351	0.2928

Table 3: MAE error of different proportions of simulated data.

Proportion of simulated data (%)	1000 historical ramping events	100 historical ramping events
0	69.2109	165.9904
10	67.5309	160.4726
20	64.1745	154.3719
30	59.3285	143.1178
40	54.7197	120.9242
50	52.8801	100.6431
60	48.7161	86.6431
70	45.3877	73.4235
80	44.6338	77.5469
90	45.9218	81.3524

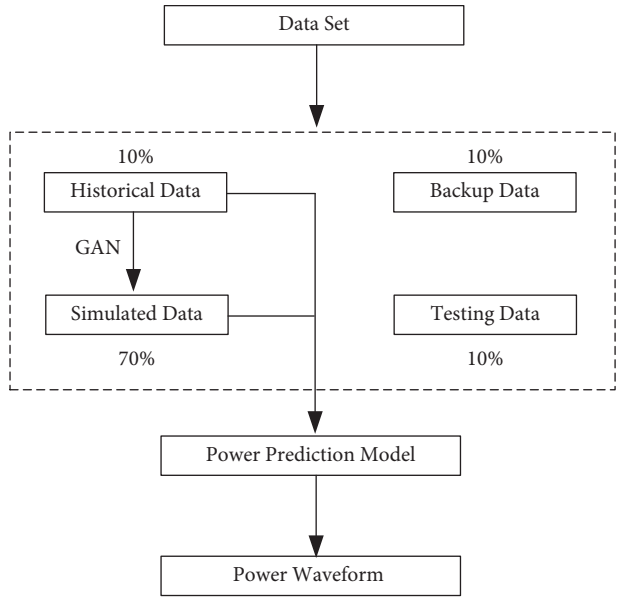

Figure 6: Flowchart of data input.

the fluctuation of power prediction and improve the accuracy of prediction.

4.6. Comparions with Other Papers. Table 6 shows four typical wind power ramping predictions of three wind farms in four quarters. It can be perceived that the prediction error in spring and autumn is slightly higher than that in summer, and the biggest error is found in winter. The results show that the Generative Adversarial Network can significantly improve the accuracy of wind power ramping prediction. The prediction accuracy is basically unaffected by seasons.

LSTM with GAN is compared to other traditional algorithms in this paper, including K-Means-LSTM, SSA-ELM, and LSTM without GAN. The results are shown as Figures 13 and 14. The MAE of four seasons and different

Table 4: Prediction evaluation of ramping events.

Model		Without GAN			With GAN		
		PR (%)	RR (%)	CSI (%)	PR (%)	RR (%)	CSI (%)
Wind farm A	LSTM	89.8406	87.2340	79.4014	99.1935	98.7952	98.0080
	SVR	78.9675	83.2661	68.1518	94.5783	90.9266	86.4220
	BP	74.0458	79.6715	62.2793	90.1639	85.2713	78.0142
	Elman	75.7752	78.9899	63.0645	88.0859	90.3808	80.5357
Wind farm B	LSTM	89.1837	90.4762	81.5299	99.0020	99.3988	98.4127
	SVR	78.4314	80.1603	65.6814	96.8815	93.7626	91.0156
	BP	78.1513	77.1784	63.4812	94.4000	92.9134	88.0597
	Elman	79.2017	75.0996	62.7288	93.5354	94.8770	89.0385
Wind farm C	LSTM	87.1845	93.3472	82.0841	87.1845	98.5915	97.4155
	SVR	80.7767	78.7879	66.3477	80.7767	94.3888	90.7514
	BP	75.9295	80.0000	63.8158	75.9295	94.7368	87.9699
	Elman	73.2824	76.6467	59.9064	73.2824	92.8571	82.4275

Table 5: MAE with and without Generative Adversarial Network.

	Model	Without GAN	With GAN
Wind farm A	LSTM	165.9904	72.3265
	SVR	171.4142	94.8642
	BP	210.6367	131.0226
	Elman	187.8891	150.1042
Wind farm B	LSTM	73.1862	48.0482
	SVR	78.6676	59.3349
	BP	86.0760	52.7223
	Elman	90.0243	60.0757
Wind farm C	LSTM	83.9457	48.4726
	SVR	119.5956	69.6969
	BP	126.6824	82.8137
	Elman	141.9668	88.1768

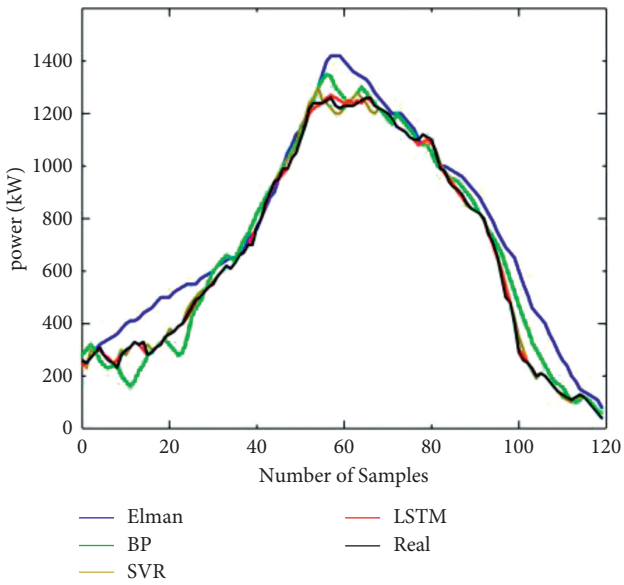

Figure 7: Comparison of power waveform prediction of wind farm A.

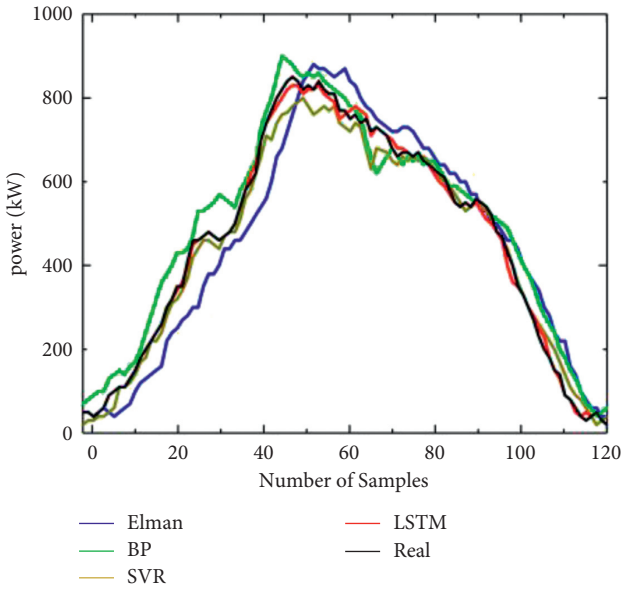

Figure 8: Comparison of power waveform prediction of wind farm B.

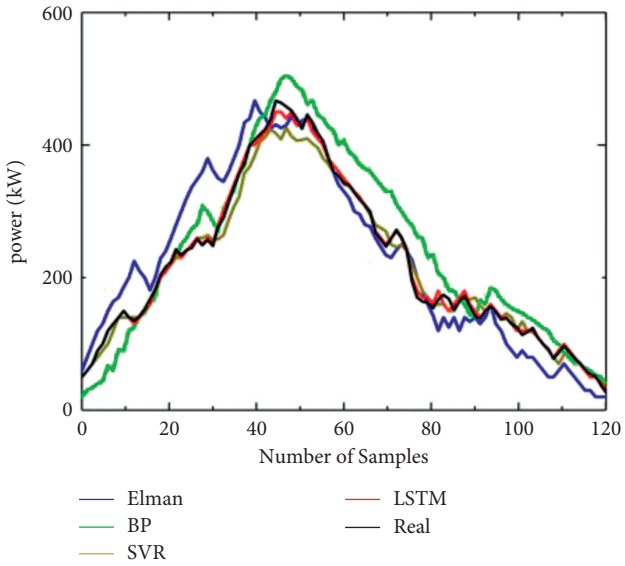

Figure 9: Comparison of power waveform prediction of wind farm C.

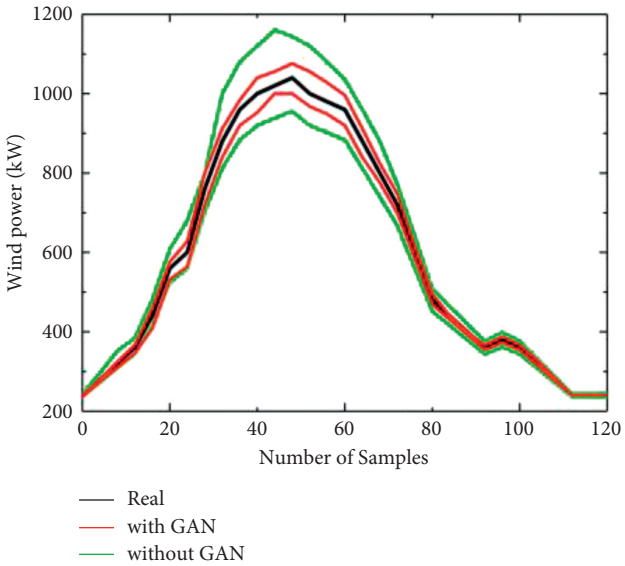

Figure 10: Prediction with wind farm of 90% confidence.

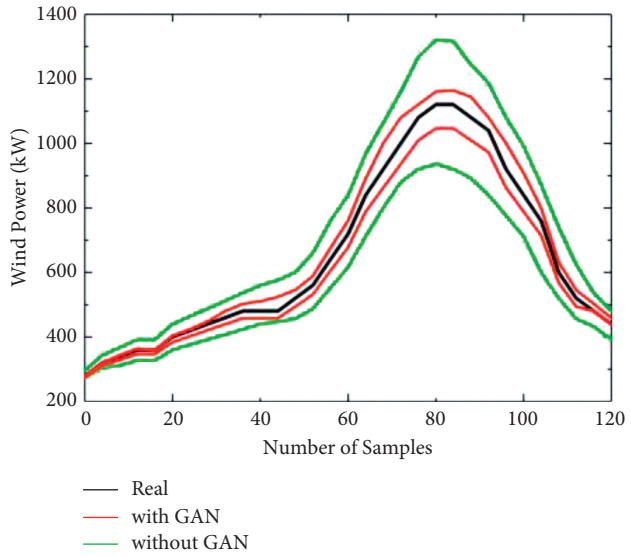

Figure 11: Prediction with wind farm of 80% confidence.

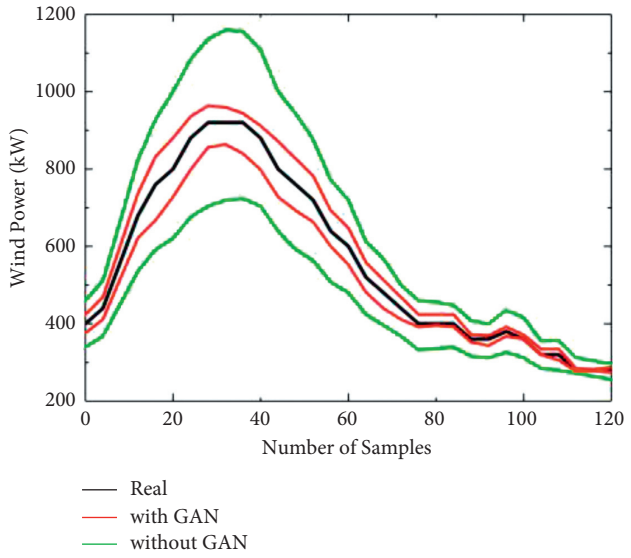

Figure 12: Prediction with wind farm of 70% confidence.

Table 6: MAE of different seasons.

Model		Without GAN	With GAN
Wind farm A	Spring	165.9904	72.3265
	Summer	182.5894	79.5515
	Autumn	193.8891	86.1748
	Winter	209.4882	92.4013
Wind farm B	Spring	73.1862	48.0482
	Summer	80.5042	52.8502
	Autumn	87.1613	58.2543
	Winter	93.4275	62.0625
Wind farm C	Spring	83.9457	48.4726
	Summer	92.3427	53.3986
	Autumn	99.5356	58.7349
	Winter	106.9321	62.5075

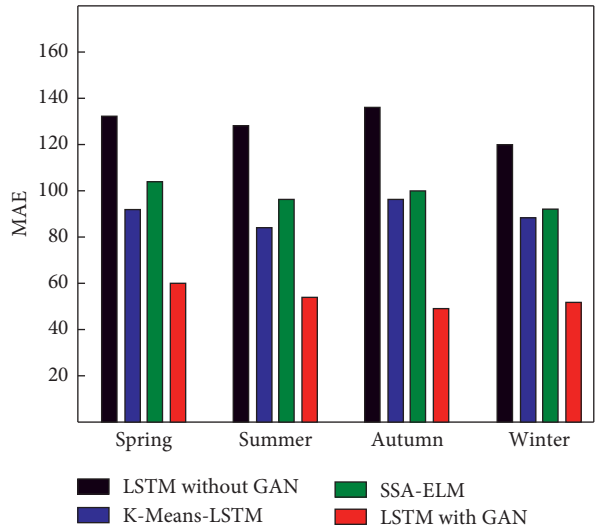

Figure 13: MAE of four seasons in the insufficient data source.

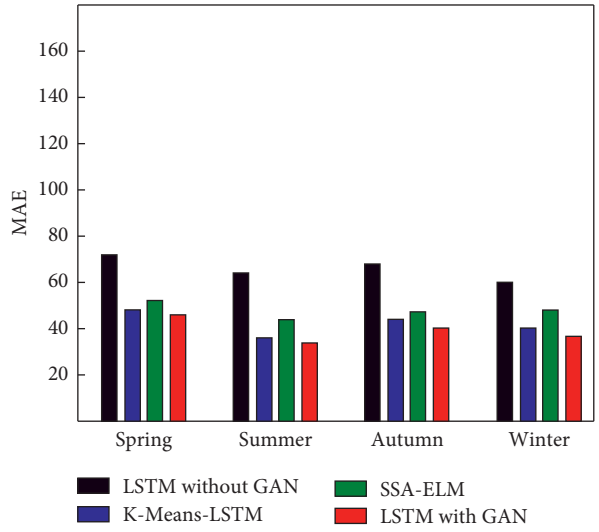

Figure 14: MAE of four seasons in the sufficient data source.

data sources is calculated, respectively, and the results are shown below. It can be seen from the table that the prediction accuracy of the algorithm based on Generative Adversarial Network is significantly higher than other algorithms when there are few data sources.

5. Conclusion

In this paper, a wind power ramping prediction model based on Generative Adversarial Network (GAN) is proposed. In light of the problems of insufficient historical data samples and low accuracy of ramping prediction in wind farms, the Generative Adversarial Network is employed to create high-reliability simulated ramping images, which enriches the database and improves the prediction accuracy. Through the simulation experiment of historical data of wind farms in Northwest China, the feasibility and superiority of the proposed model are verified. The main work of this paper can be summarized as follows:

(1) Based on its definition, valid ramping events are extracted from wind power data. According to the waveform characteristics of seven ramping events and the three weather characteristics of wind speed, temperature, and humidity, a historical ramping feature set is constructed.

(2) A method based on Generative Adversarial Network is proposed to generate data. Taking the historical ramping feature set as the input of the model, the simulated data are produced through the generator and then the discriminator determines whether the

data type is historical or simulated. Through adversarial training, the similarity level of simulated data is continuously improved. Highly similar simulated data can be used to expand the historical ramping database.

(3) The similarity between the simulated data and the historical data is calculated quantitatively, and the influence of errors in simulated data on the prediction result is analyzed. Experiments show that the simulated data are highly similar to the historical ones, and the best prediction effect is obtained when the proportion is between 70% and 80%.

(4) An evaluation system for the prediction of ramping events has been established. The ramping prediction model is evaluated from two aspects: the prediction accuracy of ramping events and the prediction accuracy of power waveform. Taking the historical data of wind farms in Northwest China as the sample, the proposed model is compared with the prediction models of SVR, BP, and Elman neural network to verify its superiority. Through different confidence levels and prediction evaluation in different seasons, it is confirmed that the generation of adversarial network algorithm can improve the accuracy of ramping prediction.

Data Availability

The data used to support the findings of this study were supplied by Hao Wang under license and so cannot be made freely available. Requests for access to these data should be made to Hao Wang (610897616@qq.com).

Conflicts of Interest

The author declares that there are no conflicts of interest.

Acknowledgments

This is a project supported by Scientific Research Fund of Zhejiang Provincial Education Department (Y202147365).

References

[1] S. A. Vargas, G. R. T. Esteves, P. M. Maçaira, B. Q. Bastos, F. L. Cyrino Oliveira, and R. C. Souza, "Wind power generation: a review and a research agenda," *Journal of Cleaner Production*, vol. 218, pp. 850–870, 2019.

[2] Z. Zonghe Gao, J. Jian Geng, K. Kaifeng Zhang et al., "Wind power dispatch supporting technologies and its implementation," *IEEE Transactions on Smart Grid*, vol. 4, no. 3, pp. 1684–1691, 2013.

[3] C. Zhang, *Research on some issues of short-term wind speed forecasting for wind farms*, Ph.D. thesis, Southeast University - Department of Law & Justice, Nanjing, China, 2017.

[4] L. Chun, F. Gaofeng, and W. Weisheng, "Combined prediction model of wind farm output power," *Power System Technology*, vol. 33, no. 13, pp. 74–79, 2009.

[5] W. Xie, P. Zhang, R. Chen, and Z. Zhou, "A nonparametric bayesian framework for short-term wind power probabilistic forecast," *IEEE Transactions on Power Systems*, vol. 34, no. 1, pp. 371–379, 2019.

[6] E. Oh and H. Wang, "Reinforcement-Learning-Based energy storage system operation strategies to manage wind power forecast uncertainty," *IEEE Access*, vol. 8, pp. 20965–20976, 2020.

[7] B. S. Qin, "Research of the wind speed and power forecasting bangsed on the actual measured date," M. S. thesis, Department Northeast Electric Power University, Jilin, China, 2018.

[8] A. Khosravi, S. Nahavandi, and D. Creighton, "Prediction intervals for short-term wind farm power generation forecasts," *IEEE Transactions on Sustainable Energy*, vol. 4, no. 3, pp. 602–610, 2013.

[9] Y. Liu, J. Shi, Y. Yang, and W.-J. Lee, "Short-term wind-power prediction based on wavelet transform-support vector machine and statistic-characteristics analysis," *IEEE Transactions on Industry Applications*, vol. 48, no. 4, pp. 1136–1141, 2012.

[10] C. M. Huang, C. J. Kuo, and Y. C. Huang, "Short-term wind power forecasting and uncertainty analysis using a hybrid intelligent method," *IET Renewable Power Generation*, vol. 11, no. 5, pp. 678–687, 2017.

[11] F. Shahid, A. Khan, A. Zameer, J. Arshad, and K. Safdar, "Wind power prediction using a three stage genetic ensemble and auxiliary predictor," *Applied Soft Computing*, vol. 90, Article ID 106151, 2020.

[12] H. Zheng and A. Kusiak, "Prediction of wind farm power ramp rates: a data-mining approach," *Journal of Solar Energy Engineering*, vol. 131, no. 3, pp. 376–385, 2009.

[13] H. Zareipour, D. Huang, and W. Rosehart, "Wind power ramp events classification and forecasting: a data mining approach," in *Proceedings of the IEEE Power & Energy Society General Meeting*, pp. 1–3, IEEE, San Diego, CA, USA, July 2011.

[14] M. Cui, J. Zhang, A. R. Florita, B.-M. Hodge, D. Ke, and Y. Sun, "An optimized swinging door algorithm for identifying wind ramping events," *IEEE Transactions on Sustainable Energy*, vol. 7, no. 1, pp. 150–162, 2015.

[15] C. Mingjian, S. Yunzhang, and K. Deping, "Prediction of wind power ramp based on sparse decomposition of atoms and BP neural network," *Automation of Electric Power Systems*, vol. 38, no. 12, pp. 6–11, 2014, in Chinese.

[16] T. Ouyang, X. Zha, and Q. Liang, "Wind power ramp events forecast method based on similarity correction," *Proceeding of the CSEE*, vol. 37, no. 2, pp. 572–580, 2017, in Chinese.

[17] L. Han, R. Zhang, X. Wang, A. Bao, and H. Jing, "Multi-step wind power forecast based on VMD-LSTM," *IET Renewable Power Generation*, vol. 13, no. 10, pp. 1690–1700, 2019.

[18] E. Erdem and J. Shi, "ARMA based approaches for forecasting the tuple of wind speed and direction," *Applied Energy*, vol. 88, no. 4, pp. 1405–1414, 2011.

[19] Z. Liu, M. Hajiali, A. Torabi, B. Ahmadi, and R. Simoes, "Novel forecasting model based on improved wavelet transform, informative feature selection, and hybrid support vector machine on wind power forecasting," *Journal of Ambient Intelligence and Humanized Computing*, vol. 9, no. 6, pp. 1919–1931, 2018.

[20] Y. Zhang, H. Sun, and Y. Guo, "Wind power prediction based on PSO-SVR and grey combination model," *IEEE Access*, vol. 7, pp. 136254–136267, 2019.

[21] J. Naik, S. Dash, P. K. Dash, and R. Bisoi, "Short term wind power forecasting using hybrid variational mode decomposition and multi-kernel regularized pseudo inverse neural network," *Renewable Energy*, vol. 118, pp. 180–212, 2018.

[22] R. Ak, Y.-F. Li, V. Vitelli, and E. Zio, "Adequacy assessment of a wind-integrated system using neural network-based interval predictions of wind power generation and load," *International Journal of Electrical Power and Energy Systems*, vol. 95, pp. 213–226, 2018.

[23] Y. He, Q. Xu, J. Wan, and S. Yang, "Short-term power load probability density forecasting based on quantile regression neural network and triangle kernel function," *Energy*, vol. 114, pp. 498–512, 2016.

[24] H. Zang, Z. Liang, M. Guo, Z. Qian, Z. Wei, and G. Sun, "Short-term wind speed forecasting based on an EEMD-CAPSO-RVM model," in *Proceedings of the IEEE PES Asia Pacific Power & Energy Engineering Conference (APPEEC)*, pp. 439–443, Xi'an, China, October 2016.

[25] X.-W. Mi, H. Liu, and Y.-F. Li, "Wind speed forecasting method using wavelet, extreme learning machine and outlier correction algorithm," *Energy Conversion and Management*, vol. 151, pp. 709–722, 2017.

[26] J. Yan, C. Xu, Y. Liu, S. Han, and L. Li, "Short-term wind power prediction method based on wind speed cloud model in similar day," *Automation of Electric Power Systems*, vol. 42, no. 6, pp. 53–59, 2018.

[27] O. Abedinia, M. Bagheri, M. S. Naderi, and N. Ghadimi, "A new combinatory approach for wind power forecasting," *IEEE Systems Journal*, vol. 14, no. 3, pp. 4614–4625, 2020.

[28] Y. Liu, L. Guan, C. Hou et al., "Wind power short-term prediction based on LSTM and discrete wavelet transform," *Applied Sciences*, vol. 9, no. 6, p. 1108, 2019.

[29] S.-X. Wang, M. Li, L. Zhao, and C. Jin, "Short-term wind power prediction based on improved small-world neural network," *Neural Computing & Applications*, vol. 31, no. 7, pp. 3173–3185, 2019.

[30] G. L. Ji, Y. Yuan, and J. H. Huang, "Combined model based on EEMD-HS-SVM for short-term wind power prediction," *Renewable Energy Resources*, vol. 35, no. 8, pp. 1121–1228, 2017.

[31] J. Dowell and P. Pinson, "Very-Short-Term probabilistic wind power forecasts by sparse vector autoregression," *IEEE Transactions on Smart Grid*, vol. 7, no. 2, 2016.

[32] F. Shahid, A. Zameer, A. Mehmood, and M. A. Z. Raja, "A novel wavenets long short term memory paradigm for wind power prediction," *Applied Energy*, vol. 269, Article ID 115098, 2020.

[33] R. Yu, J. Gao, M. Yu et al., "LSTM-EFG for wind power forecasting based on sequential correlation features," *Future Generation Computer Systems*, vol. 93, pp. 33–42, 2019.

[34] Z. Chang, Y. Zhang, and W. Chen, "'Electricity price prediction based on hybrid model of adam optimized LSTM neural network and wavelet transform," *Energy*, vol. 187, Article ID 115804, 2019.

[35] H. Liu, X. Mi, and Y. Li, "Smart multi-step deep learning model for wind speed forecasting based on variational mode decomposition, singular spectrum analysis, LSTM network and ELM," *Energy Conversion and Management*, vol. 159, pp. 54–64, 2018.

[36] N. Lu, Y. Liu, and Y. Liu, "Application of support vector machine model in wind power prediction based on particle swarm optimization," *Discrete & Continuous Dynamical Systems—S*, vol. 8, no. 6, pp. 1267–1276, 2015.

[37] Z. Wang, B. Wang, C. Liu, and W. S. Wang, "Improved BP neural network algorithm to wind power forecast," *The Journal of Engineering*, vol. 2017, no. 13, pp. 940–943, 2017.

[38] T. Lin, R. Q. Cai, and L. Zhang, "Prediction intervals forecasts of wind power based on IBA-KELM," *Renewable Energy Resources*, vol. 36, no. 7, pp. 1092–1097, 2018.

[39] C. Wan, Z. Xu, P. Pinson, Z. Y. Dong, and K. P. Wong, "Probabilistic forecasting of wind power generation using extreme learning machine," *IEEE Transactions on Power Systems*, vol. 29, no. 3, pp. 1033–1044, 2014.

[40] H. Liu, X. Mi, and Y. Li, "An experimental investigation of three new hybrid wind speed forecasting models using multi-decomposing strategy and ELM algorithm," *Renewable Energy*, vol. 123, pp. 694–705, 2018.

[41] A. A. Abdoos, "A new intelligent method based on combination of VMD and ELM for short term wind power forecasting," *Neurocomputing*, vol. 203, pp. 111–120, 2016.

[42] S. Jianbo, W. Xiaoshan, and Z. Buhan, "Wind power range prediction based on nonparametric kernel density estimation," *Hydroelectric Energy Science*, vol. 31, no. 9, pp. 233–235, 2013.